Spora: A Journal of Biomathematics

Volume 6 Article 2

2020

A Demographic Model of an Endangered Florida Native Bromeliad (Tillandsia utriculata)

Zoe S. Brookover
Rhodes College, brozs-21@rhodes.edu

Alexandra M. Campbell
Rhodes College, camam-20@rhodes.edu

Brian D. Christman
Rhodes College, chrbd-21@rhodes.edu

Sydney L. Davis
Rhodes College, davsl-21@rhodes.edu

Erin N. Bodine
Rhodes College, bodinee@rhodes.edu

A Demographic Model of an Endangered Florida Native Bromeliad (Tillandsia utriculata)

Cover Page Footnote

The authors would like to thank Dr. Teresa Cooper for the use of her raw data from [6] which allowed for the parameterization of the model presented in this paper.

Intercollegiate Biomathematics Alliance

SPORA
A Journal of Biomathematics

ISSN 2473-3067 (Print)
ISSN 2473-5493 (Online)

A Demographic Model of an Endangered Florida Native Bromeliad, *Tillandsia utriculata*

Zoe S. Brookover[1], Alexandra M. Campbell[1], Brian D. Christman[1], Sydney L. Davis[1], Erin N. Bodine[1,*]

*Correspondence:
Dr. Erin Bodine, Department of Mathematics & Computer Science, Rhodes College, 2000 North Parkway, Memphis, TN 38112, USA
bodinee@rhodes.edu

Abstract

The large, long-lived, epiphytic bromeliad *Tillandsia utriculata* is currently listed as state-endangered in Florida due to significant population reduction from predation by an invasive weevil, *Metamasius callizona*. We have developed a novel demographic model of a population of *T. utriculata* in Myakka River State Park (MRSP) in Sarasota, Florida using a stage-structured matrix model. Analysis of the model revealed conditions for population viability over a variety of parameter scenarios. Model analysis showed that without weevil predation the minimum germination rate required for population viability is low (4–16%), and that given a viable population at structural equilibrium we would expect to find <1% of the population in flower or post-flowering each year and, at most, about 10% of rosettes with longest leaf length (LLL) > 15 cm in flower or post-flowering each year. Additionally, the model presented here provides a basis for further analyses which explore specific conservation strategies.

Keywords: Matrix projection model, *Tillandsia utriculata*, *Metamasius callizona*, population viability, germination rate

1 Introduction

The primarily neotropical plant family Bromeliaceae contains over 3,000 species of rosette-structured flowering plants, commonly known as bromeliads [3, 5]. Large, long-lived, Florida native bromeliad populations currently face potential extirpation in Florida due to heavy predation by the invasive bromeliad-eating weevil, *Metamasius callizona* (Chevrolat). First detected in Florida in 1989, *M. callizona* has decimated native bromeliad populations across the state of Florida for the last several decades [10]. Currently, 12 of the 16 native bromeliad species are imperiled due to weevil predation [10]. The damage has been so extensive that *M. callizona* has been nicknamed the "evil weevil" [13]. The three largest Florida native bromeliads, *Tillandsia utriculata* L., *Tillandsia fasciculata* Swartz, and *Guzmania monostachia* (L.) Rusby ex Mez, have experienced the most severe population declines, and their lengthy generation times have made them slow to rebound in response to rapid weevil predation. Though not federally endangered, all three species are currently listed as endangered in Florida under the 1998 Florida Administrative Code [9]. The three largest Florida native bromeliads are also tank-forming, meaning that the base of the leaves of the rosette overlap to form a tank that collects rain water. This tank provides an aquatic micro-habitat for arboreal arthropods and frogs [2, 10]. One conservation concern about the decreasing bromeliad populations is the resulting loss of aquatic micro-habitats and the myriad of species which rely on these micro-habitats [11].

Metamasius callizona utilize bromeliads throughout their life cycle. Adult weevils consume bromeliad leaves, though this causes minimal damage to the plants [10]. The primary form of damage to the plants comes from the larva stage. Adult female *M. callizona* preferentially lay their eggs in large bromeliads. Once hatched, the larvae eat the core of the bromeliad rosette, often resulting in the death of the rosette [6, 10]. The core of the rosette includes the plant's meristematic tissue which eventually convert into an inflorescence (the flowering structure of the plant) or a clonal rosette, both means of reproduction for the plant [3]. A variety of methods for controlling the spread of *M. callizona* have been considered, but all have been found to be infeasible. Chemical controls were considered and have been applied to horticultural bromeliads in nurseries, but cannot be applied in state parks and protected lands [10]. Biological control agents were considered and potential agents identified among the native bromeliad populations of Central America, but none were successful in controlling weevil predation in Florida [7, 10, 15].

[1]Department of Mathematics & Computer Science, Rhodes College, Memphis, TN

Of the three largest Florida native bromeliads, *T. utriculata* is considered most in danger of extirpation in Florida due to its distinctive life history strategy. Most bromeliads have the ability to vegetatively generate clonal rosettes, known as ramets or pups, where each rosette of the genetic individual (i.e., the genet) produces a single inflorescence. Species of rosette forming plants where each rosette produces only one inflorescence are known as monocarpic. Monocarpic rosettes which produce clonal rosettes have multiple opportunities for sexual reproduction via flowers (one opportunity per inflorescence), a life history strategy known as iteroparity. Florida *T. utriculata*, however, do not have the capability to form clonal rosettes. Each genet is comprised of a single rosette, and therefore only has a single opportunity to sexually reproduce, a life history strategy known as semelparity [3]. If the meristematic tissue of a *T. utriculata* rosette is damaged by weevil predation prior to flowering, then that individual loses its only opportunity for sexual reproduction. *Tillandsia utriculata* is only semelparous in Florida (it is iteroparous throughout the rest of its range), and is the only Florida native bromeliad that is semelparous [14]. Current conservation methods for Florida *T. utriculata* include monitoring for signs of weevil predation in state parks and preserves and treating individual rosettes with insecticide if needed, using conservation cages, and employing human-assisted seed dispersal to ensure that as many seeds as possible land in the canopy (as epiphytes seeds need to germinate on a host tree in order to have long-term survival) [2, 16]. Additionally, a conservation/recovery method currently under consideration is seed banking. This strategy involves collecting and storing some or all of the *T. utriculata* seeds produced in a given year to be dispersed and germinated in subsequent years [presented at the 2019 Florida Bromeliad Conservation Working Group at Marie Selby Botanical Gardens, Sarasota, FL].

Mathematical modeling provides a method for exploring the impact of current and future conservation/recovery methods for *T. utriculata*. However, several Florida *T. utriculata* demographic parameters such as the germination rate (i.e., the proportion of seeds produced that successfully germinate) and size-specific induction rates (i.e., the proportion of rosettes of a specific size which start producing an inflorescence each year) are currently unknown. To inform reasonable parameter ranges for the germination rate and induction rates, we develop a novel stage-structured demographic matrix projection model for a Florida *T. utriculata* population in Myakka River State Park (MRSP) in Sarasota, FL. Analysis of the model is used to determine the minimum germination rate required for population viability in the presence and absence of weevil predation, the sensitivity of the population's yearly growth rate to variation in the germination rate and the inflorescence induction rates, and the conditions for the viability of a *T. utriculata* population. The model presented here provides a basis for future analyses that explore the impact of specific conservation methods.

See the Appendix for a brief glossary of biological terms.

Table 1: *Tillandsia utriculata* information by size class determined by longest leaf length (LLL). Yearly death rates are given for no weevil predation (NWP) and with weevil predation (WWP). The green values correspond to rosettes pre-induction, while the bolded **purple** values correspond to rosettes post-induction corresponding to the coloring of the life cycle graph in Figure 1.

Size Class	**Age (yrs)**	**LLL (cm)**	**Yrly Death Rate NWP**	**WWP**
Recruit	0 – 3	0 – 5	0.7212	0.7252
Tiny	3 – 5	5 – 15	0.7212	0.7252
Small	5 – 8	15 – 30	0.5546 **0.5556**	0.5724 **0.5728**
Medium	8 – 12	30 – 50	0.5546 **0.5556**	0.5724 **0.5728**
Large	12 – 17	50 – 90	0.6206 **0.6772**	0.8076 **0.7673**
V. Large	> 17	90 – 105	0.6206 **0.6772**	0.8076 **0.7673**

2 Mathematical Model

We use a stage-structured matrix projection model to simulate the population dynamics of a Florida *T. utriculata* population. The model is constructed using the size classifications given in [8] and shown in Table 1. The size classes are determined by longest leaf length (LLL) measured in cm.

The matrix projection model is given by

$$\mathbf{x}(t+1) = \mathbf{A}\mathbf{x}(t), \tag{1}$$

where $\mathbf{A}$ is the 10×10 matrix given in Table 2 and has the following parameters: P_i is the yearly probability of an individual surviving and remaining in stage i; G_i is the yearly probability of an individual surviving and progressing to stage $i+1$; I_i is the yearly probability of an individual surviving and going through induction while remaining in the same size class; and F_i is the seed fecundity of stage i. Note, the probability of an individual in stage i surviving to the next time step is $S_i = P_i + G_i + I_i$. A seed bank class is not included because *T. utriculata*

Table 2: Matrix **A** from Equation (1).

$$\left[\begin{array}{cccccc|cccc} P_1 & 0 & 0 & 0 & 0 & 0 & F_7 & F_8 & F_9 & F_{10} \\ G_1 & P_2 & 0 & 0 & 0 & 0 & 0 & 0 & 0 & 0 \\ 0 & G_2 & P_3 & 0 & 0 & 0 & 0 & 0 & 0 & 0 \\ 0 & 0 & G_3 & P_4 & 0 & 0 & 0 & 0 & 0 & 0 \\ 0 & 0 & 0 & G_4 & P_5 & 0 & 0 & 0 & 0 & 0 \\ 0 & 0 & 0 & 0 & G_5 & P_6 & 0 & 0 & 0 & 0 \\ \hline 0 & 0 & I_3 & 0 & 0 & 0 & P_7 & 0 & 0 & 0 \\ 0 & 0 & 0 & I_4 & 0 & 0 & 0 & P_8 & 0 & 0 \\ 0 & 0 & 0 & 0 & I_5 & 0 & 0 & 0 & P_9 & 0 \\ 0 & 0 & 0 & 0 & 0 & I_6 & 0 & 0 & 0 & P_{10} \end{array}\right]$$

seeds are only viable for approximately six months after dispersal.

A life cycle graph of the model described by Equation (1) is given in Figure 1. In a life cycle graph, each stage is a node, and a loop is a path from a node to itself.

For a matrix projection model consisting of a matrix that is irreducible and primitive, we are able to use basic matrix algebra to determine the growth rate and structural equilibrium of the population.

Lemma 1. *Let* **A** *be the* 10×10 *matrix defined in Table 2. Then* **A** *is irreducible and primitive.*

Proof. Let **A** be the 10×10 matrix defined in Table 2 which is a non-negative matrix.

A non-negative matrix is irreducible if in its life cycle graph representation there exists a path from every node to every other node [4]. The life cycle graph in Figure 1 shows that there are no terminal nodes, and thus there is a path from every node to every other node. Thus, **A** is irreducible.

An irreducible matrix is primitive if the greatest common divisor of the loop lengths of its life cycle graph is 1 [4]. The life cycle graph in Figure 1 has loops of length 1, 4, 5, 6, and 7, and thus the greatest common divisor of the loop lengths is 1. Therefore, **A** is a primitive matrix. □

Theorem 1. *Let* **A** *be the* 10×10 *matrix defined in Table 2. Then there exists a simple, real, positive eigenvalue* λ_1 *that is greater in magnitude than any other eigenvalue, and its corresponding left and right eigenvectors are real and strictly positive.*

Proof. Let **A** be the 10×10 matrix defined in Table 2. By Lemma 1, **A** is irreducible and primitive. Thus, by the Perron-Frobenius Theorem, there exists a simple, real, positive eigenvalue λ_1 that is greater in magnitude than any other eigenvalue, and its corresponding left and right eigenvectors are real and strictly positive [4, 12]. □

For matrix projection models which simulate population dynamics, λ_1 (called the dominant eigenvalue) biologically represents the growth rate of the population at

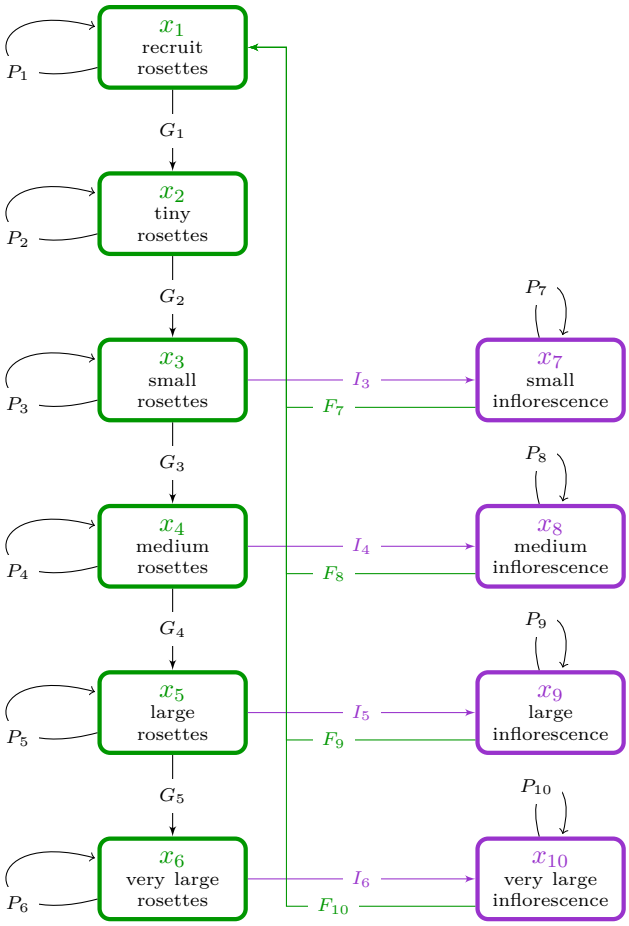

Figure 1: Life cycle graph for Equation (1). **Green** states are size classes of rosettes started from seed that are pre-induction, while **purple** states are size classes of rosettes that are post-induction. Black lines indicate growth and survival rates (G_i and P_i), **purple** lines indicate induction rates (I_i), and **green** lines indicate new rosette production from seed (i.e., fecundity values, F_i).

structural equilibrium (also known as the stable stage distribution). A population modeled by Equation (1) will be at a structural equilibrium when $\mathbf{x}(t+1) = c\mathbf{x}(t)$, where c is a fixed constant approximated by λ_1. The normalized eigenvector associated with the dominant eigenvalue represents the proportion of the population in each stage at the structural equilibrium; though the population may increase or decrease, these proportions remain constant once structural equilibrium is reached.

3 Parameter Estimation

All estimated parameter values for the model in Equation (1) are given in Table 4. Here we provide descriptions for how each value is calculated and the data that were used for calculations.

Induction Rates. The small, medium, large, and very large size classes of *T. utriculata* are able to go through induction, after which new rosette leaf production ceases and the production of the inflorescence for sexual reproduction begins. This process occurs in a rosette in stage i (for $i = 3, 4, 5, 6$) at a rate given by $I_i = \alpha\rho_i(1 - d_i)$, where α is the yearly induction rate for rosettes that have reached the minimum size for inflorescence induction (MSI), ρ_i is the probability that a rosette in stage i has reached its minimum size for inflorescence induction, and d_i is the yearly death rate of stage i (see Table 1 and note $S_i = 1 - d_i$). We assume a yearly induction rate of $\alpha = 0.4507$ which yields a probability that 95% of rosettes that have reached their MSI have gone through induction within 5 years. *Tillandsia utriculata* rosettes cannot go through induction prior to tank formation which happens around 15 cm LLL, and the maximum LLL is around 105 cm [3, 6]. Thus, we assume the distribution of sizes (denote as ℓ measures as LLL in cm) at which *T. utriculata* rosettes have reached their MSI is given by a bounded probability density functions, specifically a shifted beta distribution given by

$$B(\ell) = \begin{cases} \frac{1-\ell_{\min}}{\beta(a,b)} \sqrt{\dfrac{\ell_{\max} - \ell}{\ell_{\max} - \ell_{\min}}} & \ell_{\min} \le \ell \le \ell_{\max} \\ 0 & \text{otherwise} \end{cases} \tag{2}$$

where $\ell_{\min}$ is the smallest possible MSI, $\ell_{\max}$ is the largest possible MSI, and $\beta(a,b) = \int_0^1 t^{a-1}(1-t)^{b-1}\,dt$ is the Euler Beta function. The parameter values $\ell_{\min} = 15$ cm, $\ell_{\max} = 90$ cm, $a = 2$, and $b = 1.5$ give a beta distribution which has its peak at 65 cm and a mean value of 57.9 cm (as shown in Figure 2).

The probability that a rosette in stage i has reached its MSI is given by $\rho_i = \int_0^{\bar{\ell}_i} B(\ell)\,d\ell$, where $\bar{\ell}_i$ is the midpoint of the LLL (in cm) range for stage i; the LLL range for each size-class are given in Table 1. The parameter values $\ell_{\min} = 15$ cm, $\ell_{\max} = 90$ cm, $a = 2$, and $b = 1.5$ give probabilities $\rho_1 = \int_0^{2.5} B(\ell)\,d\ell = 0$, $\rho_2 = \int_0^{10} B(\ell)\,d\ell = 0$, $\rho_3 = \int_0^{22.5} B(\ell)\,d\ell = 0.0181$, $\rho_4 = \int_0^{40} B(\ell)\,d\ell = 0.1835$, $\rho_5 = \int_0^{70} B(\ell)\,d\ell = 0.7108$, and $\rho_6 = \int_0^{97.5} B(\ell)\,d\ell = 1$.

Table 3: Parameterizations of $B(\ell)$ from Equation (2). All parameterization use $a = 2$ with b calculated from Equation (3) given $a = 2$ and the given peak value.

Range	η	ρ_1	ρ_2	ρ_3	ρ_4	ρ_5	ρ_6
Broad 15–90 cm	75	0	0	0.0138	0.1466	0.6327	1
	70	0	0	0.0157	0.1632	0.6703	1
	65	0	0	0.0181	0.1835	0.7108	1
	60	0	0	0.0212	0.2086	0.7545	1
	55	0	0	0.0254	0.2402	0.8008	1
	50	0	0	0.0311	0.2810	0.8486	1
	45	0	0	0.0395	0.3347	0.8960	1
	40	0	0	0.0523	0.4074	0.9393	1
	35	0	0	0.0738	0.5081	0.9736	1
	30	0	0	0.1143	0.6488	0.9937	1
Low 15–60 cm	50	0	0	0.0395	0.3957	1	1
	45	0	0	0.0491	0.4568	1	1
	40	0	0	0.0637	0.5354	1	1
	35	0	0	0.0877	0.6371	1	1
	30	0	0	0.1319	0.7659	1	1
	25	0	0	0.2296	0.9090	1	1
High 45–90 cm	80	0	0	0	0	0.3957	1
	75	0	0	0	0	0.4568	1
	70	0	0	0	0	0.5354	1
	65	0	0	0	0	0.6371	1
	60	0	0	0	0	0.7659	1
	55	0	0	0	0	0.9090	1

Since the true underlying distribution of MSI values is unknown, in our model analysis we consider multiple parameterizations of $B(\ell)$ to capture the different possible qualitative distributions of MSI values within the *T. utriculata* population (see Table 3). The peak of $B(\ell)$ is given by

$$\eta = \frac{(a-1)(\ell_{\max} - \ell_{\min})}{a + b - 2} + \ell_{\min}. \tag{3}$$

All parameterizations in Table 3 use $a = 2$ and calculate b from Equation (3) to obtain the desired peak. Three different MSI ranges are considered: Broad with $\ell_{\min} = 15$ cm and $\ell_{\max} = 90$ cm, Low with $\ell_{\min} = 15$ cm and $\ell_{\max} = 60$ cm, and High with $\ell_{\min} = 45$ cm and $\ell_{\max} = 90$ cm. In the Low MSI range, the probability that a rosette has reached its MSI once it has reached the large size class (LLL 50–90 cm) is 100%. In the High MSI range, rosettes must reach at least the large size

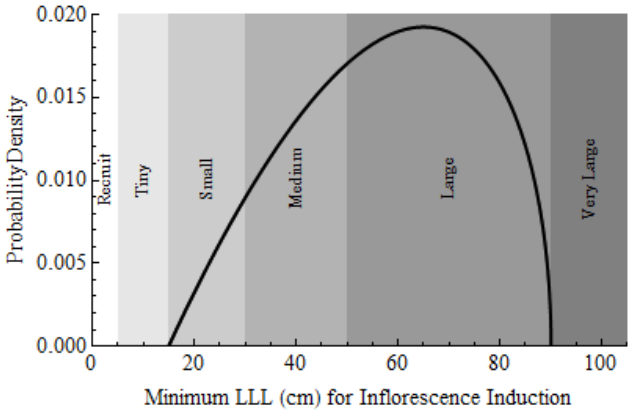

Figure 2: Probability density function $B(\ell)$ given in Equation (2) with delineation of size classes shown, where ℓ is the longest leaf length (LLL).

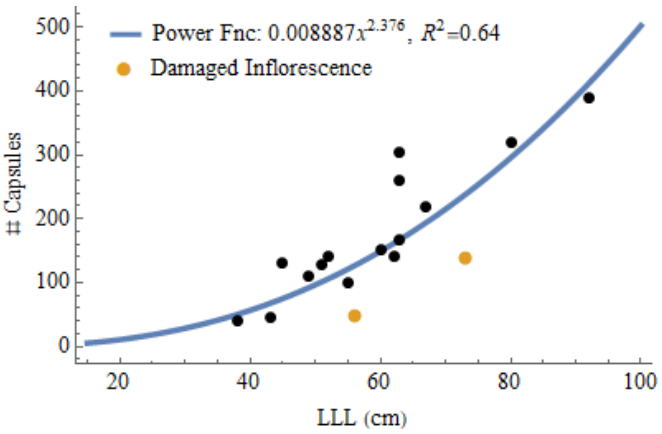

Figure 3: Capsule count data collected from 17 *T. utriculata* at Tropiflora Inc., Sarasota, FL on 11 June 2019 correlated to longest leaf length (LLL).

class (LLL 50–90 cm) before it reaches its MSI. We have included the High MSI range because there is anecdotal evidence [personal communication with T. Cooper, 2019] that some *T. utriculata* rosettes do not start to produce an inflorescence until they have reached the large or very large size class. The High MSI range considers a whole population of such individuals.

Survival & Growth Rates. Recall that the probability that a rosette in stage i survives to the next time step is $S_i = P_i + G_i + I_i = 1 - d_i$. The yearly death rate for each size class, d_i, is calculated for no weevil predation (NWP) and with weevil predation (WWP) by fitting an exponential decay function $e^{-d_i/12}$, using a least squares method, to the survival distribution data from [6, Chapter 5] (see death rate columns in Table 1). In [6, Chapter 5], survival data for multiple species of *Tillandsia* (including *T. utriculata*, *T. fasciculata*, *T. balbisiana*) are analyzed collectively. Using the raw data, we rederived the survival rates for *T. utriculata* only.

For stages with $G_i > 0$, the probability of a rosette surviving from one year to the next and growing into the next size class is $G_i = (S_i - I_i)/a_i$ where a_i is the average number of years a rosette spends in the size class corresponding to stage i (see the age column of Table 1). The probability of a rosette surviving from one year to the next and remaining in the stage is calculated as $P_i = S_i - G_i - I_i$.

Seed Fecundity. The inflorescence of a single *T. utriculata* rosette is branched with each branch producing one or more capsules. Each capsule is comprised of three chambers. For *T. utriculata*, data collected by Bennett [1] showed a mean of 79.1 seeds per chamber (SD 21.1, $n = 20$). On 11 June 2019, we collected data on the number of capsules per inflorescence for 17 *T. utriculata* at Tropiflora, Inc. in Sarasota, FL. The collected data are shown in Figure 3. Note, two inflorescences had damage along one or more of the branches, yielding lower capsule counts. Using a least-squares regression, we fit a power function to the capsule count data,

$$c(\ell) = 0.008887\ell^{2.376}, \tag{4}$$

where ℓ is the LLL (cm) and c is the number of capsules per inflorescence (and thus per rosette). Assuming 79.1 seeds per chamber and the relationship between LLL and capsule count given in Equation (4), we estimate the relationship between LLL and seed count as

$$f(\ell) = (3)(79.1)(0.008887)\ell^{2.376}, \tag{5}$$

where ℓ is the LLL (cm) and f is the number of seeds per inflorescence (and thus per rosette).

Fecundity values are calculated as $F_i = g \cdot f(\bar{\ell}_i)$, where g is the germination rate (which we vary in our model analysis), and $\bar{\ell}_i$ is the midpoint of the LLL (in cm) size range for stage i. For the size class which have the potential to produce seeds (i.e., $i = 3, 4, 5, 6$), $f(\bar{\ell}_3) = 3,442$; $f(\bar{\ell}_4) = 13,507$; $f(\bar{\ell}_4) = 51,051$; and $f(\bar{\ell}_6) = 112,183$.

4 Model Analysis Methods

For the model in Equation (1), the yearly population growth rate, generational growth rate, generation time, and structural equilibrium are calculated over multiple parameterizations of **A**. This captures the potential variation of unknown parameters, specifically the germination rate (g) and the probability that a rosette in stage i has reached its MSI (ρ_i). Additionally, the sensitivity of the yearly population growth rate with respect to each

Table 4: Parameterization of Equation (1) for a MRSP Florida *T. utriculata* population. Parameter values ρ_i are given in Table 3, and values for g are varied from 0.01 to 1.

i	Class	S_i	P_i	G_i	I_i	F_i
1	recruit, from seed	0.2788	0.1859	0.0929	—	—
2	tiny, from seed	0.2788	0.1394	0.1394	—	—
3	small, from seed	0.4454	0.2945	0.1473	$0.4507 \cdot \rho_3 \cdot S_3$	—
4	medium, from seed	0.4454	0.3064	0.1022	$0.4507 \cdot \rho_4 \cdot S_4$	—
5	large, from seed	0.3794	0.2063	0.0516	$0.4507 \cdot \rho_5 \cdot S_5$	—
6	very large, from seed	0.3794	0.2084	—	$0.4507 \cdot \rho_6 \cdot S_6$	—
7	small with inflorescence	0.4444	0.4444	—	—	$3{,}442 \cdot g$
8	medium with inflorescence	0.4444	0.4444	—	—	$13{,}507 \cdot g$
9	large with inflorescence	0.3228	0.3228	—	—	$51{,}051 \cdot g$
10	very large with inflorescence	0.3228	0.3228	—	—	$112{,}183 \cdot g$

$S_i = P_i + G_i + I_i = 1 - d_i$, where d_i (yearly death rate of rosettes in stage i) is given in Table 1

P_i = probability of surviving and remaining in stage i

G_i = probability of surviving and progressing to stage $i+1$

I_i = probability of surviving and producing an inflorescence; remains in same size class

F_i = seed fecundity of stage i

ρ_i = probability that a rosette is stage i has reached its MSI

g = germination rate of *T. utriculata* seeds

matrix entry (a_{ij}) is calculated. The model analysis is used to determine the minimum germination rate necessary for population viability in the presence and absence of weevil predation, the sensitivity of the population's yearly growth rate to variation in the inflorescence induction rates, and the conditions under which a *T. utriculata* population, diminished by weevil predation, can rebound.

Yearly Population Growth Rate (λ_1). Given the model defined in Equation (1), the yearly population growth rate of the Florida *T. utriculata* population in Myakka River State Park is given by the dominant eigenvalue (defined as λ_1) of $\mathbf{A}$. The dominant eigenvalue was determined for varying germination rates, where $g \in \{0.00, 0.01, 0.02, \ldots, 1.00\}$ for the 22 different sets of induction rates determined by Table 3. Note λ_1 has units of years^{-1}.

Calculation of $\mathcal{R}_0$ and the Generation Time (τ). The projection matrix $\mathbf{A}$ can be decomposed into matrices $\mathbf{H}$ and $\mathbf{F}$ such that $\mathbf{A} = \mathbf{H} + \mathbf{F}$ where elements h_{ij} represent the probability that a rosette in stage j at time step t is alive and in stage i at time step $t+1$, and f_{ij} is the expected number of type i offspring produced by an individual in stage j (i.e., a fecundity value). The fundamental matrix $\mathbf{M} = (\mathbf{I} - \mathbf{H})^{-1}$ (where $\mathbf{I}$ is the identity matrix) has elements m_{ij} which represent the expected value of the number of visits to transient stage i before absorption (i.e., death) given that an individual starts in stage j [4]. The matrix $\mathbf{R} = \mathbf{FM}$ has elements r_{ij} which represent the expected lifetime production of type i offspring from rosettes starting in stage j, and the dominant eigenvalue of $\mathbf{R}$ is $\mathcal{R}_0$. The value of $\mathcal{R}_0$ represents the growth rate of the population from one generation to the next. The generation time (τ) is determined from $(\lambda_1)^\tau = \mathcal{R}_0$, i.e. $\tau = \ln \mathcal{R}_0 / \ln \lambda_1$ [4]. The generation time (τ) was determined for varying germination rates, where $g \in \{0.00, 0.01, 0.02, \ldots, 1.00\}$ for the 22 different sets of induction rates determined by Table 3. Note $\mathcal{R}_0$ has units of generations^{-1}, and τ has units of years.

Structural Equilibrium ($\mathbf{v}_1$). The normalized eigenvector corresponding to the dominant eigenvalue of $\mathbf{A}$ (denoted as $\mathbf{v}_1$) gives the proportion of the population in each stage at structural equilibrium. From this vector we can calculate what proportion of the rosettes in the population are in each size class at the structural equilibrium, and the proportion of the population which would be post-induction (and thus likely in flower) at the structural equilibrium. We define p to be the proportion of population which is post-induction at the structural equilibrium (i.e., the proportions of the population in states x_7, x_8, x_9, and x_{10}). Further, we define the visible class as the combination of pre- and post-induction classes containing small, medium, large, and very large rosettes (a total of eight states). Thus, the visible class contains all rosettes with LLL $>$ 15 cm. We then define q as the proportion of the visible class which is post-induction

at the structural equilibrium. The structural equilibrium was determined for varying germination rates, where $g \in \{0.00, 0.01, 0.02, \ldots, 1.00\}$ for the 22 different sets of induction rates determined by Table 3.

Sensitivity of λ_1 to Parameter Variation. The sensitivity of the dominant eigenvalue of $\mathbf{A}$ to small changes in element a_{ij} of $\mathbf{A}$ is the rate of change $\frac{\partial \lambda_1}{\partial a_{ij}}$. The sensitivity matrix of $\mathbf{A}$ is a matrix of the same dimension of $\mathbf{A}$ (i.e., 10×10) denoted as $\mathbf{S}$ where

$$s_{ij} = \frac{\partial \lambda_1}{\partial a_{ij}}.$$

It can be shown (see Chapter 9 of [4] for derivation) that

$$\mathbf{S} = \frac{\mathbf{w}_1 \mathbf{v}_1^T}{\mathbf{w}_1^T \mathbf{v}_1}, \tag{6}$$

where $\mathbf{w}_1$ and $\mathbf{v}_1$ are the left and right eigenvectors, respectively, corresponding to λ_1, and the superscript T denotes the transpose. Both $\mathbf{w}_1$ and $\mathbf{v}_1$ have dimensions 10×1. The sensitivity matrix was calculated for varying germination rates, where $g \in \{0.00, 0.01, 0.02, \ldots, 1.00\}$ for the 22 different sets of induction rates determined by Table 3.

5 Results

We considered how the yearly growth rate (λ_1), the proportion of the population that is post-induction at structural equilibrium (p), the proportion of the visible class that is post-induction at structural equilibrium (q), the generation time (τ), and the sensitivity of the yearly growth rate to the parameters of $\mathbf{A}$ change over different germination rates $g \in \{0.00, 0.01, 0.02, \ldots, 1.00\}$ for the 22 different sets of induction rates determined by Table 3.

Impact of parameter uncertainty on λ_1, p, and q. The sensitivity of the yearly growth rate (λ_1) to changes in the germination rate (g) and peak MSI value (η) are shown as matrix plots in Figure 4. The value of λ_1 is calculated for each (g, η) pair both without weevil predation (top graph in red) and with weevil predation (bottom graph in blue). On both graphs, the thick black line indicates where $\lambda_1 = 1$. Note, the population is declining when $\lambda_1 < 1$, the population is stable when $\lambda_1 = 1$, and the population is growing when $\lambda_1 > 1$. For the MRSP *T. utriculata* population to experience yearly growth when no weevil predation is present, very low germination rates are sufficient (Table 5). This concurs with previous statements (lacking quantification) that the germination rate of *T. utriculata* is "low" [3, 14]. Additionally, the minimum germination rate increases across each MSI range category as the peak MSI (η) increases. For example, in the broad range MSI only a 4% germination rate is needed if $\eta = 30$ cm LLL, but an 9% germination rate is needed if $\eta = 75$ cm LLL. Higher germination rates are necessary for population growth when weevil predation is present, particularly for high range MSI values.

Table 5: Minimum germination rate (g) required for $\lambda_1 > 1$ by MSI range category.

MSI Range	w/o Predation	w/ Predation
Broad 15–90 cm	4–9%	6–17%
Low 15–60 cm	4–6%	5–9%
High 45–90 cm	10–16%	30–58%

For parameter sets representing populations with long-term viability (i.e., with $\lambda_1 > 1$), the proportion of the population that is post-induction at structural equilibrium (p) was at most 0.0022 without weevil predation and 0.0019 with weevil predation. Thus, at structural equilibrium we should expect to find less than 1% of the population in flower or post-flowering in a given year. The maximum value of p occurred in the Low MSI range at $\eta = 25$ cm and $g = 0.04$ without weevil predation ($g = 0.05$ with weevil predation). Over the entire (g, η) parameter space, p decreased as g increased, and decreased as η increased in all MSI range categories. As the germination rate (g) increases, it makes biological sense that the proportion of the population that is post-induction would decrease because a larger germination rate corresponds to more individuals in the smallest size classes, thus making the proportions in larger size classes (including the post-induction classes) smaller. As the peak MSI (η) increases, rosettes must survive longer to reach a post-induction size class increasing the likelihood that a rosette is removed from the population before reaching a post-induction class. Thus, we see that p decreases as η increases.

For parameter sets with $\lambda_1 > 1$, the proportion of the visible class that is post-induction at the structural equilibrium (q) was at most 0.101 without weevil predation and 0.093 with weevil predation. Thus, at structural equilibrium, we should expect to see, at most, about 10% of the visible class in flower or post-flowering in a given year. The maximum values for q occur at the same parameter sets as the maximum values for p (i.e., in the Low MSI range at $\eta = 25$ cm and $g = 0.04$ without weevil predation; $g = 0.05$ with weevil predation), and displays the same general trend of decreasing as g is increased and

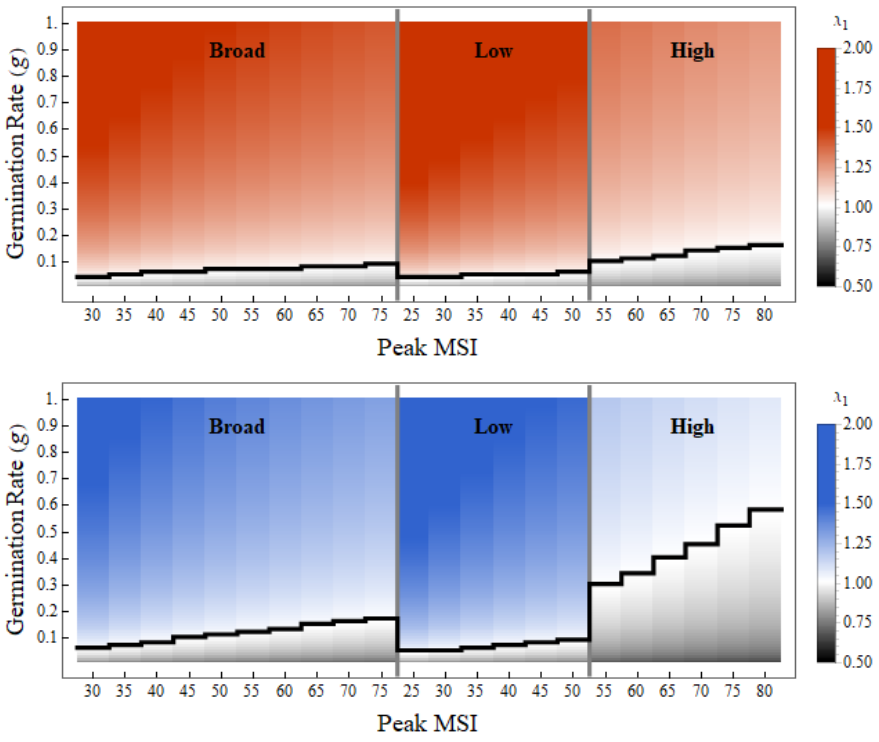

Figure 4: Matrix plots of the sensitivity of yearly growth rate (λ_1) to changes in germination rate (g) and peak MSI (η) where ■ = no weevil predation; ■ = with weevil predation.

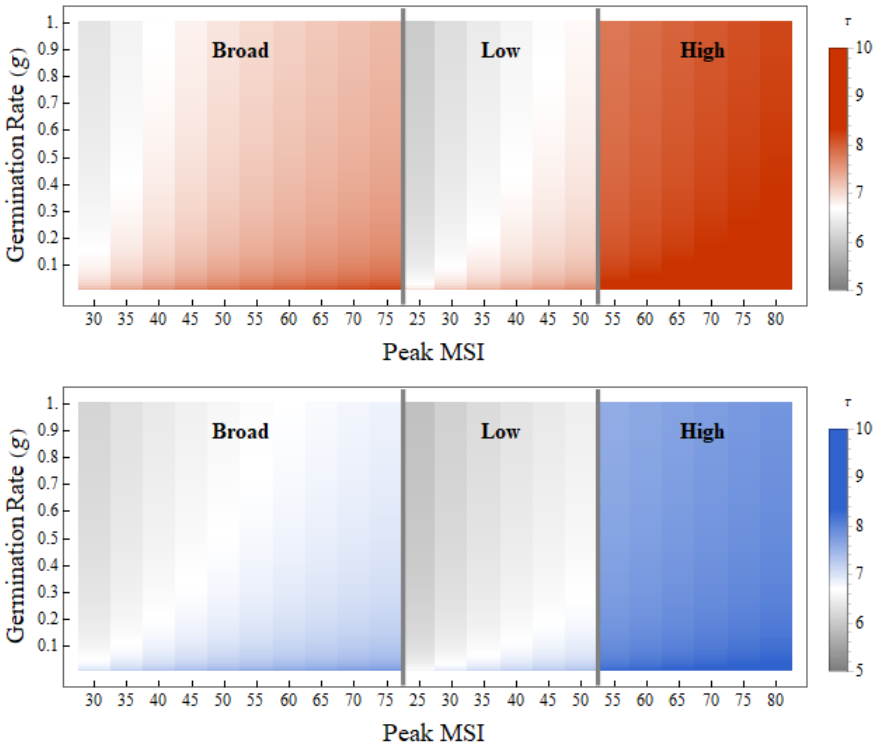

Figure 5: Matrix plots of the sensitivity of the generation time (τ) to changes in germination rate (g) and peak MSI (η) where ■ = no weevil predation; ■ = with weevil predation.

decreasing as η is increased in all MSI range categories.

Impact of parameter uncertainty on τ. Figure 5 shows the sensitivity of generation time (τ) to changes in the germination rate (g) and peak MSI value (η), in simulations both without weevil predation (top graph in red) and with weevil predation (bottom graph in blue). For our model, the generation time can be interpreted as the average time from germination to induction. Without weevil predation, generation times vary from 5.99 to 9.13 years ($[6.31, 8.29]$ yrs for Broad range MSI, $[5.99, 7.71]$ yrs for Low range MSI, $[7.78, 9.13]$ yrs for High range MSI). With weevil predation, generation times vary from 5.85 to 8.66 years ($[6.11, 7.82]$ yrs for broad range MSI, $[5.85, 7.39]$ yrs for low range MSI, $[7.55, 8.66]$ yrs for high range MSI). Note, the generation time is shortened in the presence of weevil predation for all parameter combinations of germination rate and peak MSI. For both with and without weevil predation, in the broad, low, and high categories, generation time increases with both germination rate and peak MSI.

Calculation of S for a single parameter set. The sensitivity matrix, defined in Equation (6), quantifies the sensitivity of the yearly growth rate (λ_1) to changes in entries of $\mathbf{A}$ without weevil predation. Figure 6 shows the sensitivity matrix calculated for $g = 0.20$ and $B(\ell)$ parameterized for a broad MSI range with a peak at 50 cm LLL. The matrix entries shown as dashes correspond to zero entries in $\mathbf{A}$. Each entry of $\mathbf{S}$ (denoted s_{ij}) represents the rate of change of the yearly growth rate (λ_1) given a unit increase in a_{ij}. If $s_{ij} > 0$, then λ_1 increases given a unit increase in a_{ij}; and if $s_{ij} < 0$, then λ_1 decreases given a unit increase in a_{ij}. In either case, the magnitude of s_{ij} quantifies the amount λ_1 changes given a unit increase in a_{ij}. A comparison of the relative magnitude of entries of $\mathbf{S}$ reveals the parameters of $\mathbf{A}$ to which the yearly growth rate is most sensitive. For example, Figure 6 shows that the yearly growth rate is most sensitive to small changes in the growth rates of the recruit, tiny, and small size classes (G_1, G_2, and G_3), as well as the induction rates of the small and medium size classes (I_3 and I_4); the sensitivities for these parameters range from 1.0834 to 2.3277. However, Figure 6 shows that the yearly growth rate is not very sensitive to small changes in the fecundity rates (F_7, F_8, F_9, and F_{10}); the sensitivities for these parameters range from 3.3×10^{-7} to 2.802×10^{-5}.

To determine how sensitive the yearly growth rate (λ_1) is to changes in the germination rate (g), recall that the fecundity rates (F_i) are functions of g (see Table 4). Since the yearly growth rate is a function of the entries of $\mathbf{A}$, i.e. $\lambda_1(P_1, \ldots, P_{10}, G_1, \ldots, G_5, I_3, \ldots, I_6, F_7, \ldots, F_{10})$, then by the chain rule

$$\begin{aligned}\frac{\partial \lambda_1}{\partial g} &= \frac{\partial \lambda_1}{\partial F_7}\frac{dF_7}{dg} + \frac{\partial \lambda_1}{\partial F_8}\frac{dF_8}{dg} \\ &\qquad + \frac{\partial \lambda_1}{\partial F_9}\frac{dF_9}{dg} + \frac{\partial \lambda_1}{\partial F_{10}}\frac{dF_{10}}{dg} \\ &= f(22.5)\frac{\partial \lambda_1}{\partial F_7} + f(40)\frac{\partial \lambda_1}{\partial F_8} \\ &\qquad + f(70)\frac{\partial \lambda_1}{\partial F_9} + f(97.5)\frac{\partial \lambda_1}{\partial F_{10}},\end{aligned}$$

where f is defined in Equation (5). For the sensitivity matrix shown in Figure 6 where $g = 0.20$ and $B(\ell)$ is parameterized for a broad MSI range with a peak at 50 cm LLL, $\frac{\partial \lambda_1}{\partial g} = 0.7870$. Thus, the yearly growth rate is moderately sensitive to unit increases in the germination rate compared with other model parameters.

Impact of parameter uncertainty on S. While examining the values in the sensitivity matrix shown in Figure 6 is informative, it represents only a single parameter combination of g (germination) and η (peak MSI value) for a broad MSI range. To explore the range of the sensitivity of the yearly growth rate (λ_1) to each model parameter of $\mathbf{A}$, we generated the sensitivity matrix over all combinations of germination rates $g \in \{0.00, 0.01, 0.02, \ldots, 1.00\}$ and the 22 different sets of induction rates determined by Table 3. Figures 7–11 summarize these results using box-and-whisker plots to show the range, interquartile range, and median sensitivity value for each parameter, grouped by the MSI range categories of broad, low, and high shown in Table 3. In each figure, (a) shows the sensitivities for the model parameters representing no weevil predation, and (b) shows the sensitivities for the model parameters representing the presence of weevil predation. Qualitatively, when comparing trends in sensitivities across MSI range categories, similar patterns are observed both with and without weevil predation. Quantitatively, when comparing simulations with and without weevil predation, the differences in the ranges of sensitivity values are subtle. In Figures 7–11, sensitivity rates calculated for simulations with and without weevil predation are depicted in cool tones and warm tones, respectively.

Figure 7 shows the coalesced sensitivity ranges of the yearly growth rate to all parameters of $\mathbf{A}$ grouping by parameter type: fecundity (F_i), growth rate (G_i), induction rate (I_i), and survival rate (P_i). For example, the sensitivities $\frac{\partial \lambda_1}{\partial F_7}$, $\frac{\partial \lambda_1}{\partial F_8}$, $\frac{\partial \lambda_1}{\partial F_9}$, and $\frac{\partial \lambda_1}{\partial F_{10}}$ are coalesced for each peak MSI range (broad, low, and high) and labeled as F. Figure 7 also shows the sensitivity range for the germination rate (g). Note that both plots in Figure 7 are on a logarithmic scale. The sensitivities for the fecundities are multiple orders of magnitude smaller than all

$$\mathbf{S} = \left(\begin{array}{cccccc|cccc} 0.1711 & — & — & — & — & — & 0.00001919 & 0.00002802 & 0.00000597 & 0.00000033 \\ 1.8629 & 0.1636 & — & — & — & — & — & — & — & — \\ — & 1.2419 & 0.1913 & — & — & — & — & — & — & — \\ — & — & 1.0834 & 0.1751 & — & — & — & — & — & — \\ — & — & — & 0.7747 & 0.0746 & — & — & — & — & — \\ — & — & — & — & 0.1757 & 0.0083 & — & — & — & — \\ \hline — & — & 2.3277 & — & — & — & 0.0193 & — & — & — \\ — & — & — & 1.4761 & — & — & — & 0.1105 & — & — \\ — & — & — & — & 0.4624 & — & — & — & 0.0767 & — \\ — & — & — & — & — & 0.0481 & — & — & — & 0.0094 \end{array}\right)$$

Figure 6: Sensitivity matrix calculated for $g = 0.20$ and $B(\ell)$ parameterized for a broad MSI range with a peak at 50 cm LLL without weevil predation.

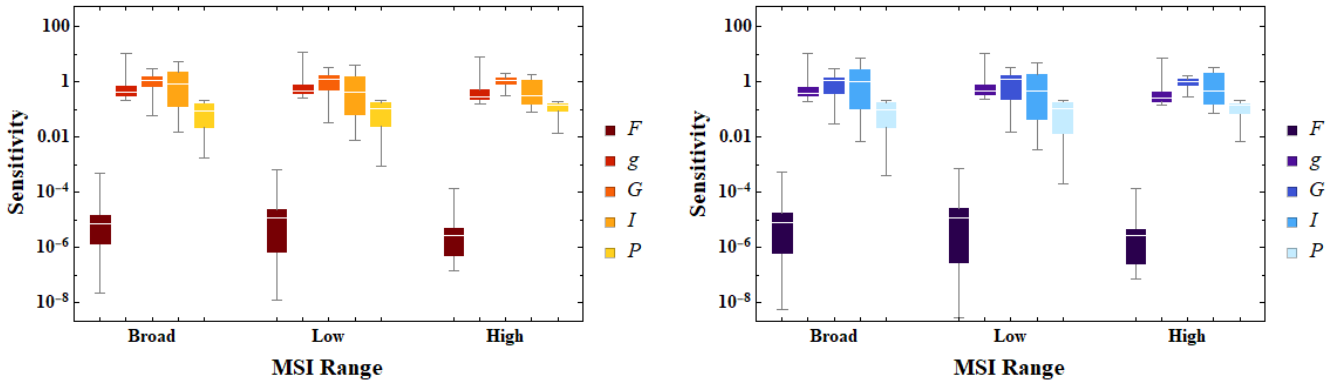

(a) No weevil predation.

(b) With weevil predation.

Figure 7: Coalesced sensitivity ranges of the yearly growth rate to all parameters of $\mathbf{S}$ grouping by parameter types fecundity (F_i), growth rate (G_i), induction rate (I_i), and survival rate (P_i), and for the germination rate (g).

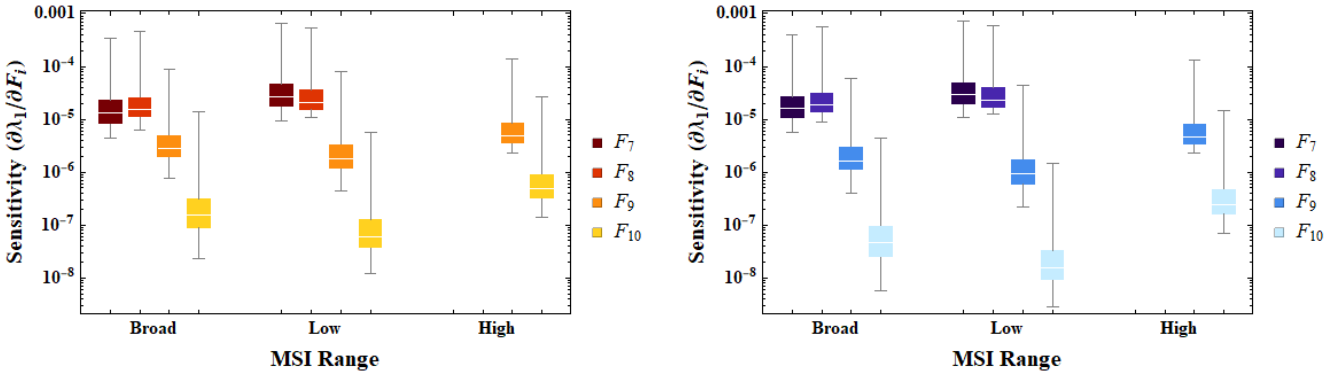

(a) No weevil predation.

(b) With weevil predation.

Figure 8: The sensitivities of the yearly growth rate to the fecundity rates for all peak MSI ranges.

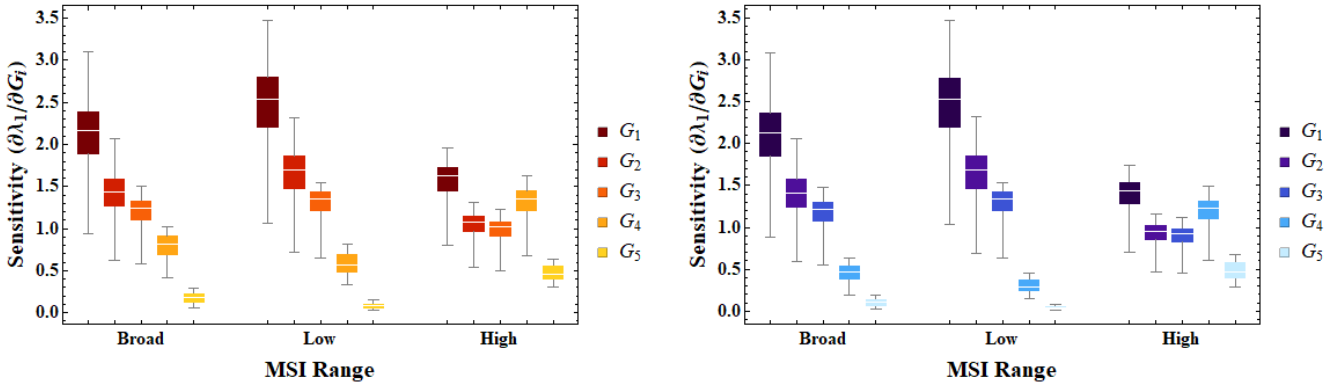

(a) No weevil predation.

(b) With weevil predation.

Figure 9: The sensitivities of the yearly growth rate to size-class specific growth rates for all peak MSI ranges.

other sensitivities, however, this is expected as the fecundity values are multiple orders of magnitude larger than the growth, survival, and induction rates. The sensitivities to the germination rate (upon which the fecundity values depend) have the largest maximum sensitivity values, and have interquartile ranges that are comparable or below the interquartile ranges for the sensitivities to growth and induction rate parameters.

Figure 8 shows the sensitivity ranges of the yearly growth rate to the fecundity values (F_i) of $\mathbf{A}$. Note that both plots in Figure 8 are on a logarithmic scale. For each of the MSI ranges, the sensitivity of the yearly growth rate decreases across the fecundity values for increasing size classes, with the exception of F_7 and F_8 in the high MSI range. In the high MSI range, $I_3 = I_4 = 0$; thus, no rosettes enter the small or medium inflorescence size classes (i.e., x_7 and x_8). Therefore, the fecundity values F_7 and F_8 are irrelevant in the high MSI range, and consequently, $\frac{\partial\lambda_1}{\partial F_7} = \frac{\partial\lambda_1}{\partial F_8} = 0$.

Figure 9 shows the sensitivity ranges of the yearly growth rate to the size-class specific growth rates (G_i) of $\mathbf{A}$. For the broad and low MSI ranges, the sensitivity of the yearly growth rate decreases across the growth rates for increasing size classes both with and without weevil predation. This pattern also holds for the high MSI range, with the exception of G_4. In the high MSI range, induction predominantly occurs in the large size class (x_5, 50–90 cm LLL). Consequently, the sensitivity of the yearly growth rate to G_4 (the growth rate from the medium to the large size class, i.e. from x_4 to x_5) is larger in the high MSI range than in the other MSI ranges.

Figure 10 shows the sensitivity ranges of the yearly growth rate to the induction rates (I_i) of $\mathbf{A}$. In simulations both with and without weevil predation, for the broad and low MSI ranges, the sensitivity of the yearly growth rate decreases across the induction rates for increasing size classes. In the high MSI range $I_3 = I_4 = 0$, and thus $\frac{\partial\lambda_1}{\partial I_3} = \frac{\partial\lambda_1}{\partial I_4} = 0$. Additionally, in the high MSI range, induction occurs from 45–90 cm LLL which is predominantly in the large size class (x_5). Thus, the yearly growth rate is substantially more sensitive to I_5 than the induction rate for the very large size class, I_6. This trend is seen both with and without weevil predation. However, the sensitivity values for simulations with weevil predation are all marginally larger than without weevil predation.

Figure 11 shows the sensitivities of the yearly growth rates to survival rates (P_i) of individuals in each stage of the model $\mathbf{A}$. The P_i values corresponding to states $x_1, \ldots, x_6$ represent survival in pre-induction states, while values corresponding to states $x_7, \ldots, x_{10}$ represent survival in post-induction states (shown in the shaded regions of Figure 11). In the pre-induction states (both with and without weevil predation), the highest sensitivity is to survival in the small size class (x_3) for the Broad and Low MSI ranges, and the medium size class (x_4) for the High MSI range. In the Broad and Low MSI ranges, rosettes must survive at least to the small size class in order to reproduce, but in the High MSI range, rosettes must survive to at least the large size class in order to reproduce. The sensitivities of the yearly growth rate to survival rates post-induction are generally lower than the sensitivities to survival rates pre-induction. In the post-induction states (both with and without weevil predation), the highest sensitivity is to the medium size class (x_8) for the Broad and Low MSI ranges, and the large size class (x_9) for the High MSI range.

6 Conclusion

Large, long-lived, Florida native bromeliad populations (including *T. utriculata*, *T. fasciculata*, and *G. monos-*

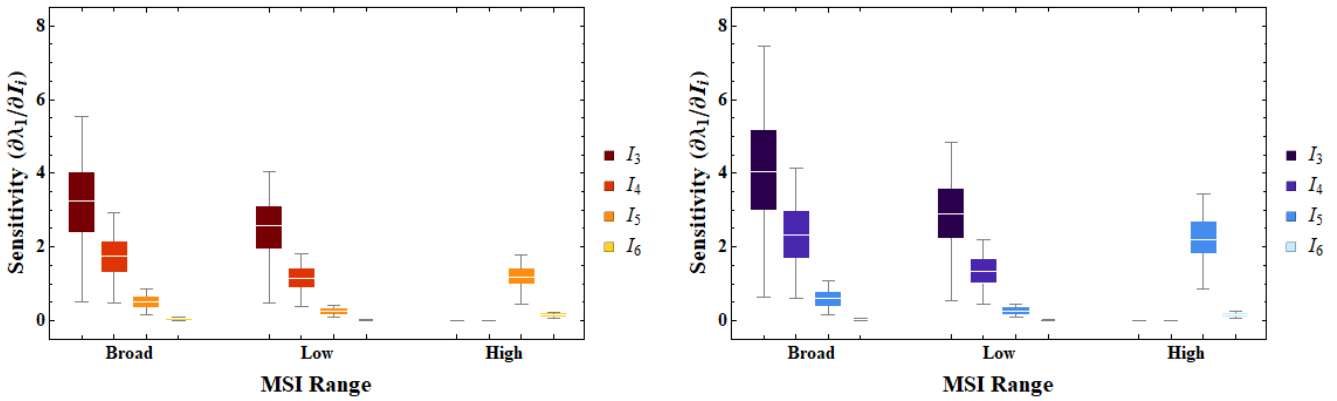

(a) No weevil predation.

(b) With weevil predation.

Figure 10: The sensitivities of the yearly growth rate to induction rates for all peak MSI ranges.

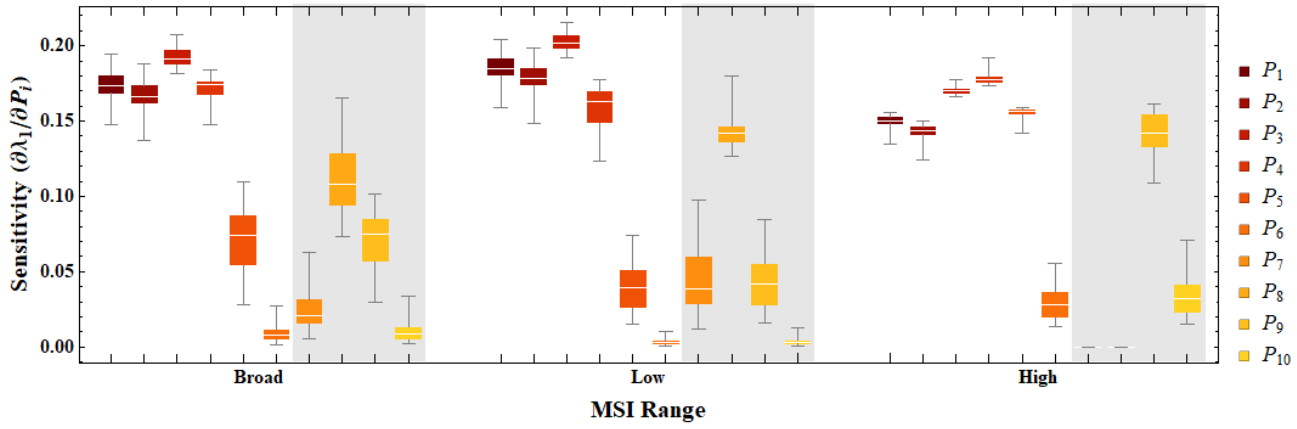

(a) No weevil predation.

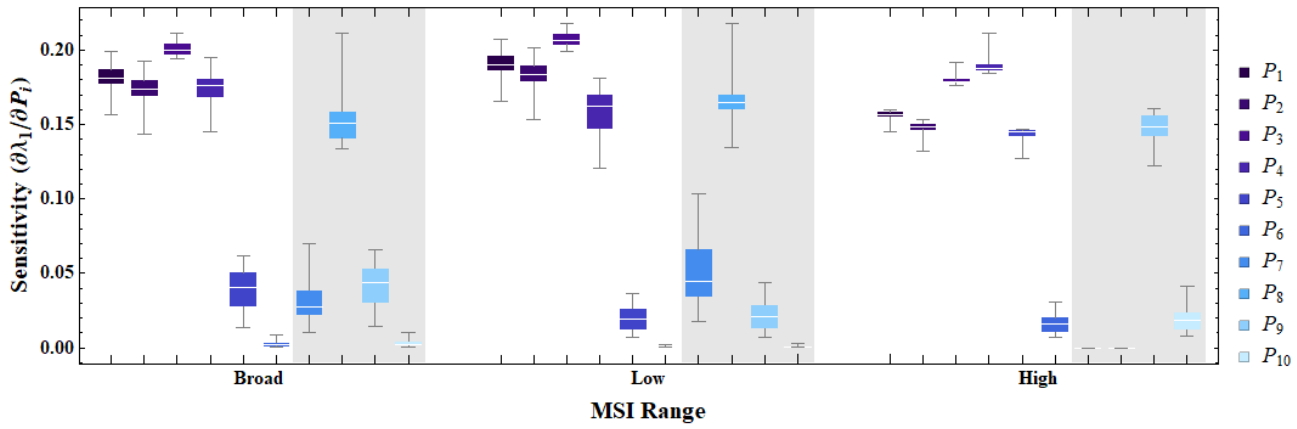

(b) With weevil predation.

Figure 11: The sensitivities of the yearly growth rate to survival rates for all peak MSI ranges. Shaded regions correspond to post-induction classes.

tachia) are facing predation from the invasive weevil, *M. callizona*. These weevils have the capacity to decimate entire bromeliad populations in Florida. Because these bromeliad species are long-lived, their populations have been slow to rebound in response to rapid weevil predation. Of these three bromeliad species, only *T. utriculata* is semelparous, and as such is at greater risk for extirpation than *T. fasciculata* and *G. monostachia* which are both iteroparous and thus have multiple opportunities for sexual reproduction.

We developed a novel demographic model of a *T. utriculata* population using a stage-structured matrix model and parameterized the model using data from a *T. utriculata* population in Myakka River State Park (MRSP) in Sarasota, FL. Given the uncertainty in some of the estimated parameter values, we evaluated the model over a range of different germination rates and MSI distributions. We used standard matrix population theory to analyze the model and determine a range of yearly growth rates, a range of generation times, a range of the proportion of the population we would expect to see in flower or post-flowering, and ranges of parameter sensitivities. The parameter sensitivities determine the parameters to which the model is most sensitive, which can be interpreted as the parameters that are most important to estimate with high accuracy.

Analysis of our model showed that without weevil predation, the minimum germination rate required for population viability is 3–15%. This result is in accordance with previous publications which classify the germination rate as "low" [3, 14]. Given that the MRSP *T. utriculata* population was viable before the introduction of the weevil, we can assume the population's germination rate is likely above 4%. Additionally, our results revealed that the sustained presence of weevil predation requires higher germination rates to support long term growth than without weevil predation. While this result is unsurprising, the utility of our model is that it quantifies the minimum germination rates required for long term population growth with and without weevil predation. Once better estimates of germination rates are established, these results can be used to assess the long term viability of the MRSP *T. utriculata* population.

Additionally, model analysis revealed the proportion of the population we would expect to see flowering or post-flowering (i.e., post-induction) when a viable population is at structural equilibrium. We would expect to find $<1\%$ of the total population post-induction and at most about 10% of visible rosettes (rosettes with LLL > 15 cm) post-induction. These values provide a way to estimate the total population size from measures of the proportion of flowering plants and provides a means of estimating the number of non-visible rosettes (<15 cm LLL). Importantly, these results are consistent in both the presence and absence of weevil predation.

Lastly, our results show that in order to accurately estimate the yearly population growth rate it is most important to have accurate estimates of the germination rate, growth rates, and induction rates with greater accuracy needed for the growth and induction rates of smaller size classes. While the germination rate and size class specific growth rates can be directly measured, the induction rates are calculated based on the MSI distributions. While the MSI is not a quantity that can be measured, it is possible a better understanding of the underlying MSI distribution of a *T. utriculata* population could be determined by studying the distribution of sizes at which individual rosettes undergo induction (assuming the longest leaf length remains fairly constant after induction).

We are currently developing an expanded version of our model to account for the multiple attempts at sexual reproduction of iteroparous bromeliads such as *T. fasciculata* and *G. monostachia*. For iteroparous species, rosettes which germinate from seed can grow at different rates than clonal rosettes which remain attached to their mother rosette for some time. These differential growth rates require that clonal rosettes be modeled as separate size classes from the rosettes started from seed. Analysis of this expanded model will allow for a comprehensive comparison of the different life-history strategies of iteroparous and semelparous species in response to weevil predation.

Additionally, due to the decimation of the *T. utriculata* populations throughout southern and central Florida, the current recovery strategy under consideration is seed-banking. This recovery strategy involves collecting and storing some or all of the seeds produced by flowering *T. utriculata* in a given year, which will then be dispersed and germinated in subsequent years. An expansion of our model that included a "seed bank" class could be used to quantify the potential impact of employing a seed-banking strategy.

Overall, damage wrought by the "evil weevil" throughout southern and central Florida over the past 30 years has been of great concern to state park and forest/ wildlife sanctuary managers, and to the broader Florida bromeliad horticultural community. Analysis of our novel demographic model provides insights into which life history parameters need to be measured with greater accuracy, and provides a launching point with regards to further understanding the population dynamics and conservation of large, long-lived bromeliads.

Author Contributions

Brookover (undergraduate), Campbell (undergraduate), Christman (undergraduate), Davis (undergraduate), and

Bodine (faculty) developed and parameterized the model, performed all model analysis, and interpreted the results. Campbell, Christman, Davis, and Bodine collected the capsule count data used to generate Equation (4).

Acknowledgments

The authors would like to thank Dr. Teresa Cooper for the use of her raw data from [6] which allowed for the parameterization of the model presented in this paper. Additionally, we would like to thank Tropiflora, Inc. for the use of their facilities and plants in collecting the capsule count data used to generate Equation (4). We would like to thank Dr. Brad Oberle for assisting in the collection of capsule count data at Tropiflora, Inc. Lastly, we would like to thank Drs. Rachel Jabaily and Brian Sidoti for general discussions about the biology and life history of the epiphytic bromeliads of Florida.

Appendix

A brief glossary of relevant biological terms.

germination the time at which a rosette sprouts from a seed

induction the time at which new leaf production ceases and the building of the inflorescence begins

inflorescence the reproductive structure of a plant include stalk, bracts, and flowers

iteroparity a life history strategy where a genetic individual has multiple chances at sexual reproduction

monocarpy producing one inflorescence per rosette

meristematic tissue the reproductive tissues of plants

semelparity a life history strategy where a genetic individual has only one chance at sexual reproduction

References

[1] Bennett, B. C. (1988). A comparison of life history traits in selected epiphytic and saxicolous speices of *Tillandsia* (Bromeliaceae) in Florida and Peru. Doctoral Dissertation, University of North Carolina, Chapel Hill.

[2] Bennett, B. C. (1989). The Florida bromeliads: *Tillandsia utriculata*. *Journal of the Bromeliad Society*, 39(6): 265–271.

[3] Benzing, D. H. (2000). *Bromeliaceae: Profile of an Adaptive Radiation*. Cambridge, UK: Cambridge University Press.

[4] Caswell, H. (2001). *Matrix Population Models: Construction, Anlysis, and Interpretation*, 2^{nd} Edition. Sunderland, MA: Sinauer Associates, Inc.

[5] Christenhusz, M. J. M. and Byng, J. W. (2016). The number of known plants species in the world and its annual increase. *Phytotaxa* 261(3): 201–217. doi:10.11646/phytotaxa.261.3.1

[6] Cooper, T. M. (2006). Ecological and demographic trends and patterns of *Metamasius callizona* (Chevrolat), an invasive bromeliad-eating weevil, and Florida's native bromeliads. Master's thesis, University of Florida.

[7] Cooper, T. M., Frank, J. H., Cave, R. D., Burton, M. S., Dawson, J. S., and Smith, B. W. (2011). Release and monitoring of a potential biological control agent, *Lixadmontia franki*, to control an invasive bromeliad-eating weevil, *Metamasius callizona*, in Florida *Biological Control* 59(3): 319–325. doi:10.1016/j.biocontrol.2011.08.005

[8] Cooper, T. M. (2016). Save Florida's Bromeliads: A Method for Conserving Florida's Airplants. University of Florida, Institute of Food and Agricultural Science. `https://entomology.ifas.ufl.edu/frank/savebromeliads/conservation-method.html` *Accessed: 02 May 2019.*

[9] Florida Administrative Code. (1998). Plants in the Preservation of Native Flora of Florida Act. Chapter 5B-40.0055, Regulated Plant List. `https://www.flrules.org/gateway/ChapterHome.asp?Chapter=5B-40` *Accessed: 03 Jan 2020.*

[10] Frank, H. and Cave, R. (2005). *Metamasius callizona* is destroying Florida's native bromeliads. In: Hoddle, M.S. (Ed.), Second International Symposium on Biological Control of Arthropods, USDA Forest Service Publication FHTET-2005-08. USDA Forest Service, 91–101. `https://www.bugwood.org/arthropod2005/`

[11] Frank, J. H. and Fish, D. (2008). Potential biodiversity loss in Florida bromeliad phytotelmata due to *Metamasius callizona* (Coleoptera: Dryophthoridae), an invasive species. *Florida Entomologist* 91(1): 1–8. doi:10.1653/0015-4040(2008)091[0001:PBLIFB]2.0.CO;2

[12] Kot, M. (2001). *Elements of Mathematical Ecology.* Cambridge, UK: Cambridge University Press.

[13] Larson, B. and Frank, J. H. (2013). Mexican Bromeliad Weevil (suggested common name), Metamasius callizona (Chevrolat) (Insecta: Coleoptera: Curculionidae) Featured Creatures from the Entomology and Nematology Department, UF/IFAS Extension. EENY-161 (IN318) `http://entnemdept.ufl.edu/creatures/`

[14] Luther, H. E. and Benzing, D. H. (2009). Native Bromeliads of Florida. Sarasota, FL: Pineapple Press, Inc.

[15] Sauzo, A., Arismendi, N., Frank, J. H., and Cave, R. D. (2006). Method for continuously rearing *Lixadmontia franki* (Diptera: Tachinidae), a potential biological control agent of *Metamasius callizona* (Coleoptera: Dryophthoridae). *Florida Entomologist* 89(3): 348–353. doi:10.1653/0015-4040(2006)89[348:MFCRLF]2.0.CO;2

[16] Save Florida's Bromeliads Conservation Project. (2019). Updates. `https://www.savebromeliads.com/sfbcp-updates` *Accessed: 03 Jan 2019.*